High-field MRS – Teaching Session II

JOSEF PFEUFFER

Max-Planck Institute for Biological Cybernetics
Department Physiology of Cognitive Processes, Tübingen, Germany
josef.pfeuffer@tuebingen.mpg.de

Introduction

What is a *high* magnetic field? For horizontal *in vivo* MR systems using small animals like mice or rats, magnets of field-strengths as high as 11.7 T/ 31 cm (500 MHz) are available. *Vertical* microimaging systems operate up to 17.6 T/ 89 mm (750 MHz) and will reach in near future 21.2 T/ 105 mm (900 MHz). For research in humans the highest field currently available is 9.4 T / 65 cm (400 MHz), while in the clinical environment the highest field is 3-4 T / 95 cm (130-170 MHz).

MR spectroscopy (MRS) evolved rapidly over the last decades, and it is now an important tool in chemical and biological research focused on molecular composition, structure, and dynamics. Experiments initially conducted in cells and cell extracts, are now carried out in living animals and humans. Similarly, MRS applications in clinical diagnosis are growing steadily. The importance of field strength in such applications cannot be overemphasized: "increasing the magnetic field strength increases spectral resolution also for 1H NMR, which can lead to more than linear sensitivity gains", Fig.1 (Gruetter *et al.*, 1998b).

The several fold improved sensitivity at high fields enables the detailed quantitative study of both metabolic and neural signaling processes, as well as of their perturbations during disease.

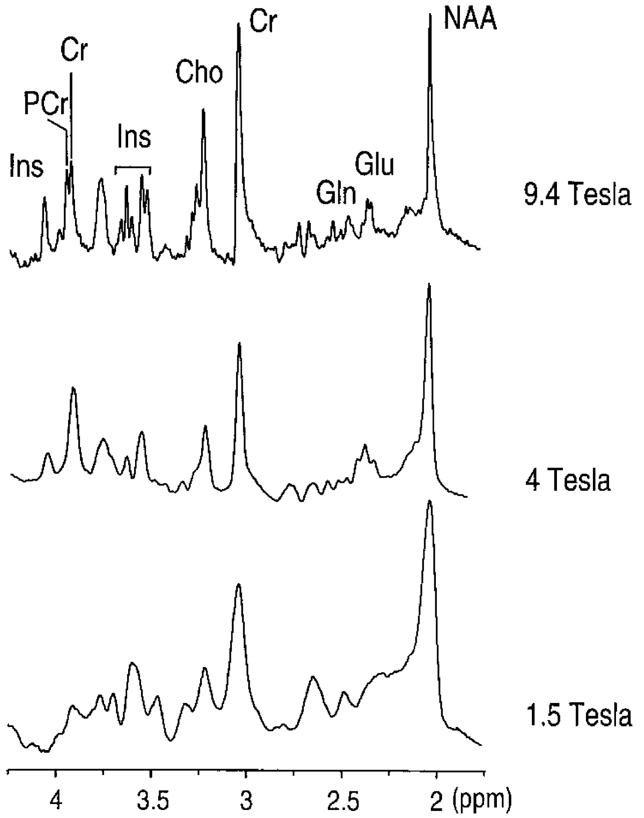

Figure 1. Comparison of increases in spectral resolution with magnetic field strength. The stack plot shows corresponding spectra from 27-ml volumes in the human occipital lobe at 1.5 T (bottom) and 4 T (middle) and a 1-ml spectrum from dog brain acquired at 9.4 T (top). Note the apparent decrease in singlet linewidths at the NAA, Cr, and Cho positions, which is direct and unequivocal evidence for increased spectral resolution *in vivo*. From (Gruetter *et al.*, 1998b).

Technical Issues

Significant improvements in signal-to-noise ratio are the most notable effects of the technical developments of *in vivo* MRS studies at high fields (Ugurbil *et al.*, 2000).

SNR gains may be a linear (e.g. ^{1}H) or even a quadratic function of field-strength, depending on several competing factors (Ugurbil *et al.*, 2003).

In the human brain, SNR comparisons for ^{1}H suggested an approximately 1.6 – 2-fold gain in sensitivity achievable at 7 T compared to 4 T (Vaughan *et al.*, 2001).

SNR data at 4.7, 11 and 17.6 T of enriched ^{17}O-water demonstrated a quadratic increase with field strength, see Fig. 2 (Thelwall *et al.*, 2003). High fields will therefore allow improved spatial and/or temporal resolution in ^{17}O-CSI of metabolically produced $H_2{}^{17}O$.

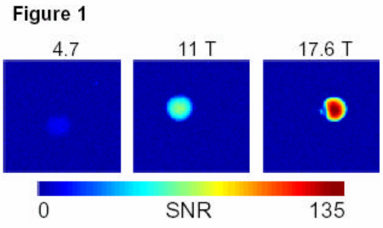

Figure 1 – *in vitro* $H_2{}^{17}O$-enriched phantom SNR plots at 4.7, 11 and 17.6 Tesla.

Table 1 – ^{17}O T_1, T_2, and SNR measurements at 4.7, 11 and 17.6 Tesla, acquired from *in vitro* samples.

Figure 2 – *in vivo* rat brain ^1H localiser images and ^{17}O CSI datasets. 4.7 T CSI data scaled by a factor of 5 cf. 11 T data.

Table 1

B_0	T_1 (ms)	T_2 (ms)	Relative SNR
4.7 T	5.93 ± 0.09	4.23 ± 0.17	0.197
11 T	5.93 ± 0.04	4.68 ± 0.08	1
17.6 T	6.05 ± 0.01	4.32 ± 0.07	2.02

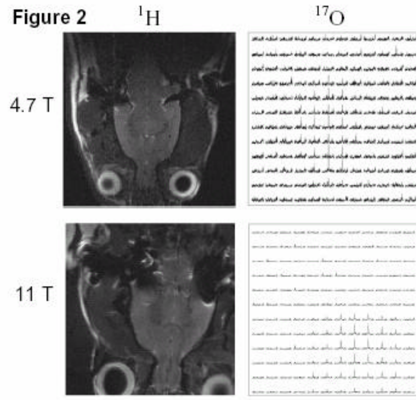

Figure 2. *In vivo* detection of $H_2{}^{17}O$ produced metabolically from $^{17}O_2$ gas has been proposed to monitor tissue oxygen consumption rate. The short T_1 of ^{17}O allows a high degree of signal averaging per unit time. We measured ^{17}O T_1 and T_2 and performed SNR measurements at 4.7, 11 and 17.6 T. ^{17}O CSI datasets at natural abundance $H_2{}^{17}O$ concentrations were acquired from *in vivo* rat brain at 4.7 and 11 T. ^{17}O T_1 and T_2 were unaffected by B_0, the increased SNR afforded by high fields will allow improved spatial and/or temporal resolution in ^{17}O CSI of metabolically produced $H_2{}^{17}O$. From (Thelwall *et al.*, 2003).

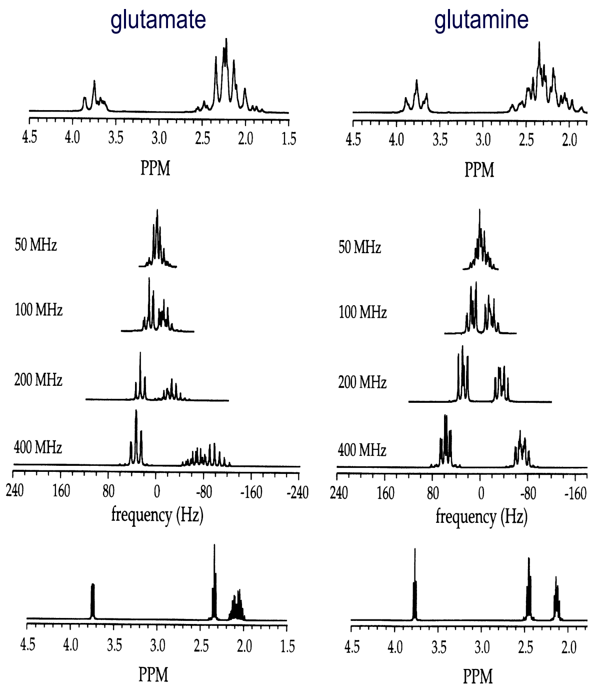

Figure 3. Magnetic field dependence of coupling patterns. From (de Graaf *et al.*, 1998).

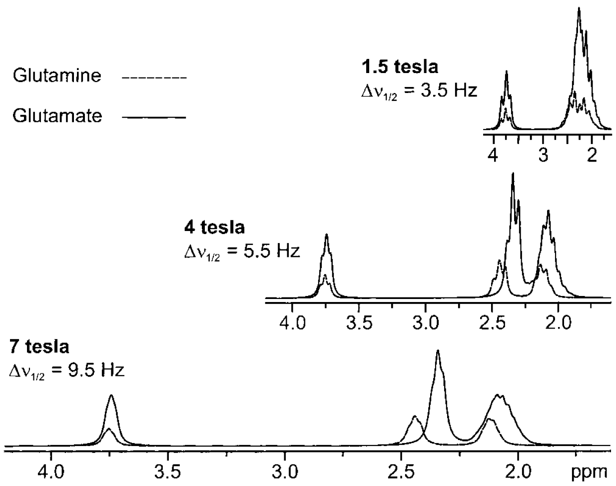

Figure 4. Simulated 1H NMR spectra of glutamine and glutamate at different magnetic field strengths. Linewidths ($\Delta\nu_{1/2}$) corresponded to values typical for very well shimmed volumes of the human brain. The concentration ratio [Glu]/[Gln] was set to 3. Frequency scale (Hz) is identical in all three spectra. From (Tkac *et al.*, 2001).

MRS at high field benefits further from an *improved spectral resolution* due to increased chemical shift dispersion and reduced higher-order coupling effects. Sensitivity *and* resolution improvements were experimentally demonstrated comparing field strengths from 1.5T to 9.4T (Gruetter *et al.*, 1998b).

In Fig. 3, the magnetic field dependence of glutamate (left) and glutamine (right) is shown in simulated ^1H spectra from 50 to 400 MHz (top to bottom). These metabolites and similarly GABA, glucose, and taurine have large second-order effects, since the J coupling constants are similar to chemical shift differences (de Graaf *et al.*, 1998).

Similarly, resonances of glutamine and glutamate ^1H NMR spectra can be better separated at increasing magnetic field strengths; typically higher fields than 4 T are necessary for a separate quantification, see Fig. 4 (Tkac *et al.*, 2001).

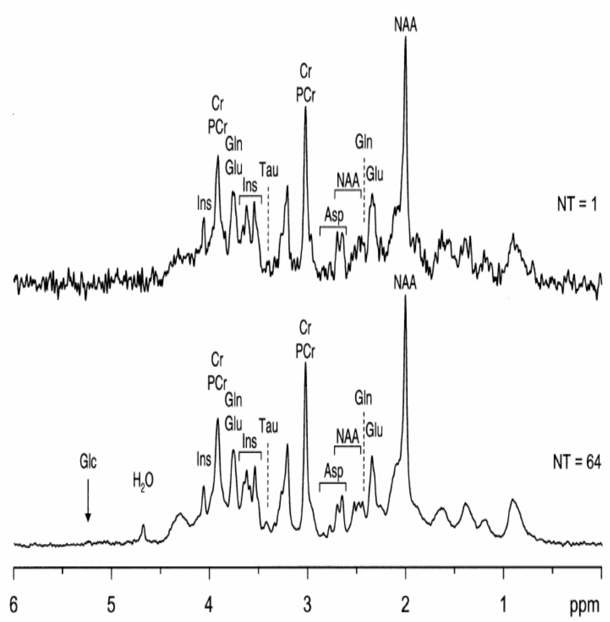

Figure 5. In vivo 1H NMR spectra of human brain (occipital gray matter) measured at 7 T by a STEAM sequence with VAPOR water suppression using a quadrature transmit/receive surface RF coil. Single shot spectrum, number of transients NT = 1 (top trace), averaged spectrum, NT = 64 (bottom trace). TE 6 ms, TM 32 ms, TR 5 s, VOI 8 mL. After Gaussian multiplication (gf = 0.1) of FID and FT only zero-order phase correction applied. From (Tkac *et al.*, 2001).

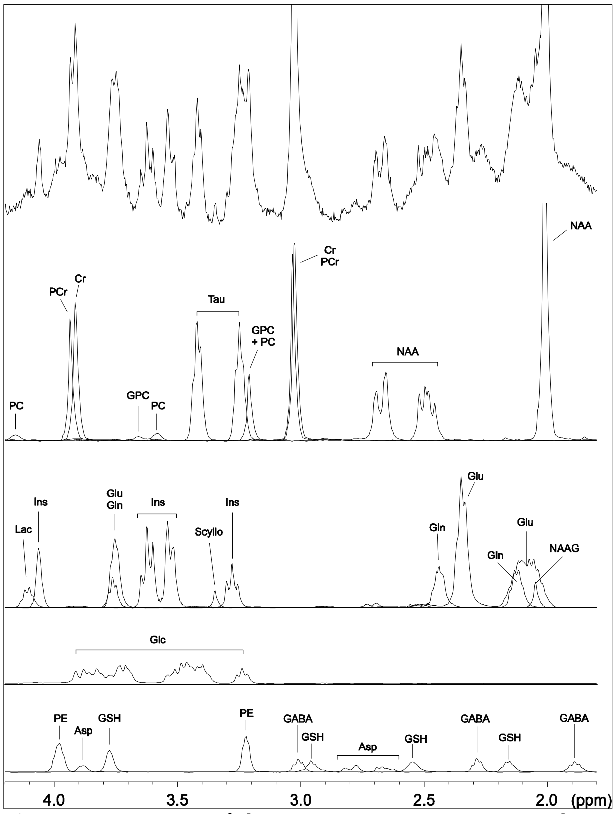

Figure 6. Comparison of the *in vivo* 1H NMR spectrum in the rat brain at 9.4 T (top) to 1H NMR metabolite model spectra. TE 2 ms, TR 6 s, 512 scans, 63-µL volume. From (Pfeuffer *et al.*, 1999b).

An important prerequisite for quality MRS is *optimal, reproducible shimming* to provide the narrowest possible *in vivo* line-widths, clearest peak separation, and increased sensitivity. Automated algorithms like FASTMAP or FLATNESS are available for shimming 1^{st}, 2^{nd}, and 3^{rd}-order contributions in a localized volume or a slice (z-shim), respectively (Gruetter, 1993; Gruetter *et al.*, 2000; Glover, 1999; Chen *et al.*, 2004).

Selected high-field applications

Excellent sensitivity of ^{1}H MRS in the human brain was shown at 7 T even with single-shot spectra, see Fig. 5 (Tkac *et al.*, 2001). At 9.4 T in the rat, up to 18 metabolites could be quantified, see Fig. 6 (Pfeuffer *et al.*, 1999b).

Localized ^{13}C MRS in the human visual cortex (4 T) and rat (9.4 T) has demonstrated its capacity to monitor glutaminergic neurotransmission, see Fig. 7 (Gruetter *et al.*, 2000; Gruetter *et al.*, 1998a; Pfeuffer *et al.*, 1999a; Henry *et al.*, 2003b; Henry *et al.*, 2003a). Moreover, oxygen consumption rate can be calculated from ^{13}C turnover. Spectacular spectra from multiple carbons of various amino acids and neurotransmitters reveal the power to obtain detailed metabolic information and study reaction-dynamics *in vivo* (Gruetter, 2002; Gruetter *et al.*, 2003).

Recent ^{17}O chemical shift imaging represents a promising new high-field application: from ^{17}O turnover of inhaled oxygen and injected water, the oxidative metabolism in the mitochondria ($CMRO_2$) was measured directly, see Fig. 8 (Zhu *et al.*, 2001; Zhu *et al.*, 2002).

Further developments and applications of ^{1}H chemical shift imaging (CSI) were steadily increasing in the last years, taking advantage of the sensitivity gains at higher magnetic field (Pan *et al.*, 1998; Pan *et al.*, 2000; van Dorsten *et al.*, 2004; Scheenen *et al.*, 2004; Dreher *et al.*, 2002; Dreher *et al.*, 2003; Mayer *et al.*, 2004; Hiba *et al.*, 2003; Hiba *et al.*, 2004). High-resolution CSI in the monkey brain at 7 T with ~1.5 mm in-plane resolution approached recently the spatial dimensions of the cortical thickness (1.5-1.7 mm in the monkey) - metabolite concentrations could be quantified separately in gray and white matter, see Fig. 9 (Juchem *et al.*, 2004).

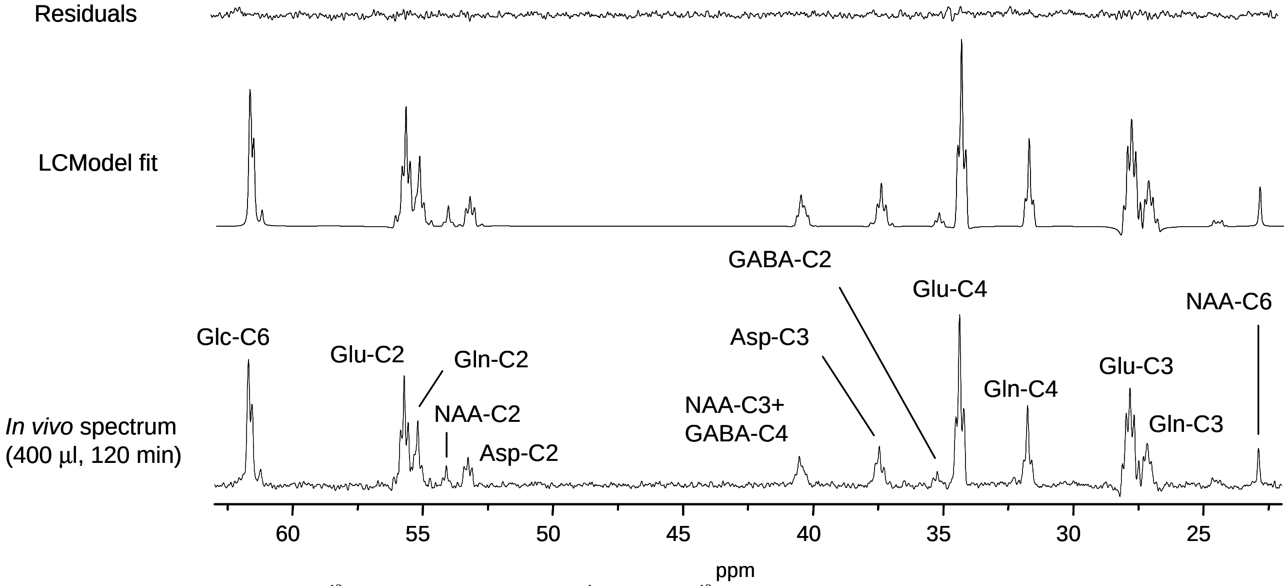

Figure 7. LCModel fit of an *in vivo* ^{13}C NMR spectrum. (bottom) ^{1}H-localized ^{13}C spectrum acquired in vivo from the rat brain 5 h after starting an infusion of [1,6-^{13}C2] glucose (2816 scans, TR 2.5 s). (middle) Fit obtained with LCModel using prior knowledge of chemical shifts and J-coupling values and (top) residuals. Only the expansion from 22 to 63 ppm is shown. From (Henry *et al.*, 2003a).

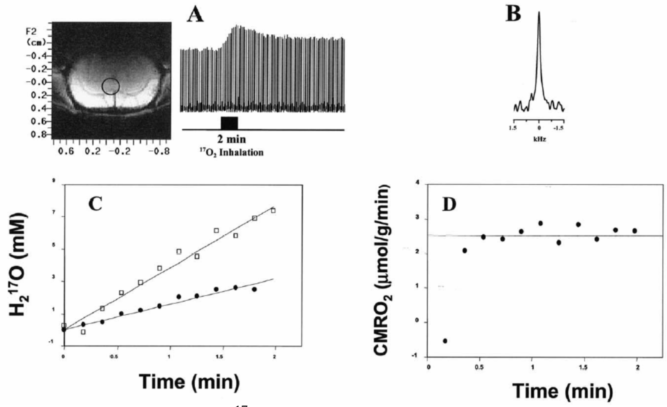

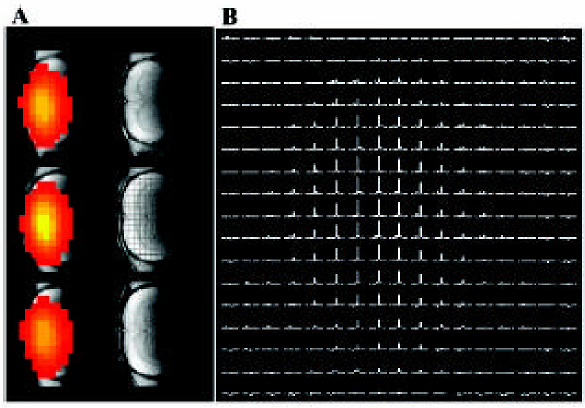

Figure 8 (left). Cerebral $H_2{}^{17}O$ spectra from one representative voxel (0.1 ml voxel size) as indicated by the circle in the anatomic image (left insert) acquired before (natural abundance), during and after a 2-min $^{17}O_2$ inhalation. ^{17}O spectrum of natural abundance $H_2{}^{17}O$ in the rat carotid artery blood obtained using the implanted RF coil before inhalation of $^{17}O_2$ (B) and time course (C) of ^{17}O MR signals during inhalation of $^{17}O_2$. (D) Plot of the calculated $CMRO_2$ values using the complete modeling as a function of inhalation time. **Figure 8 (right).** 3D ^{17}O brain images of natural abundance $H_2{}^{17}O$ from three adjacent slices (*Left*, color images) and corresponding anatomical images (*Right*, gray images) in the coronal orientation from a representative rat. (*B*) Chemical shift image of natural abundance $H_2{}^{17}O$ from *Middle* as shown in *A*. From (Zhu *et al.*, 2002).

Figure 9. High-resolution ^{1}H CSI of metabolites from gray vs. white matter in the monkey visual cortex using a vertical 7 T / 60 cm MR system. Spatial in-plane resolution was below 1.5 mm. SNR and spectral/spatial resolution were high enough to distinguish GM and WM reliably via their metabolite concentrations.

(a)(b) Anatomical FLASH (axial, coronal) showing WM and GM areas; zoomed CSI FOV to the right.

(c) S/N map from LCModel fit. The WM (white contour) and vessel region (left horizontal black contour) show lower metabolite signals than the voxels in GM.

(d)(e) Map of NAA/NAAG and Glu/Gln concentrations (relative to 8 mM for Cr/PCr).

(f) CSI FOV with selected WM and GM tissue.

(g) Metabolite concentration histograms for Cr/PCr, NAA/NAAG and Glu/Gln in GM and WM. Metabolite concentrations were significantly higher in GM ($p<1e-5$). Ratios of NAA/NAAG vs. Cr/PCr and Glu/Gln vs. Cr/PCr were consistent with the literature.

Experimental parameters: STEAM: TE/TM 10ms, TR 3s, NA 42, VOI 17x17x2mm^3. CSI: 2D phase encoding, matrix size 13x13. Post-processing: smooth Gaussian filtering (62% at the edges), zero-filling to 27x27. Quantification: voxelwise with LCModel, Cramér-Rao lower bounds were (10.3 ± 3.3)% for NAA/NAAG and (16.4 ± 8.2)% for Glu/Gln. From (Juchem *et al.*, 2004)

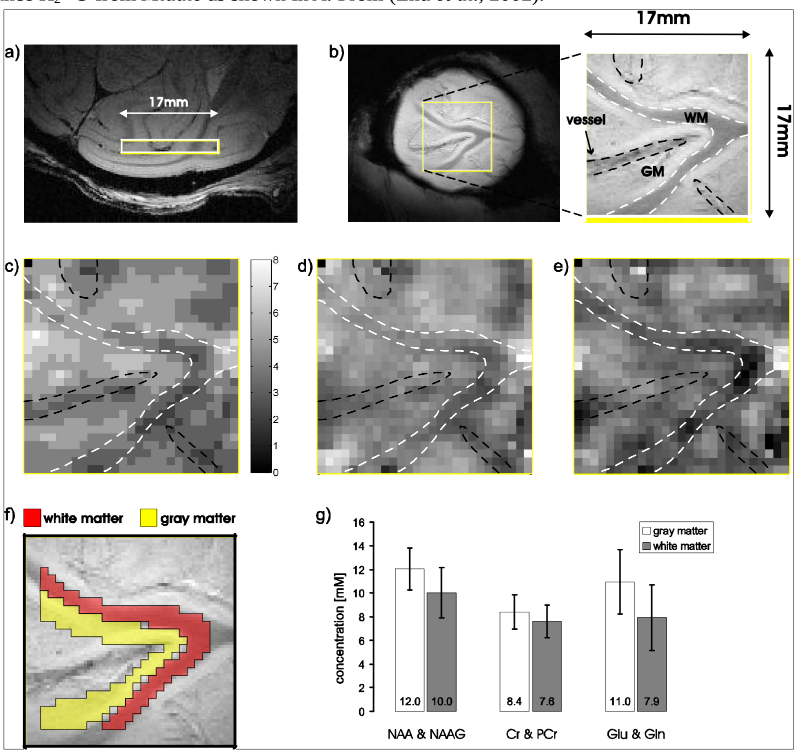

References

Chen, Z., Li, S. S., Yang, J., Letizia, D., and Shen, J. 2004. Measurement and automatic correction of high-order B0 inhomogeneity in the rat brain at 11.7 Tesla. *Magn Reson Imaging* **22:** 835-842.

de Graaf, R. A., and . 1998. In vivo NMR spectroscopy: principles and techniques. *John Wiley & Sons*.

Dreher, W., Geppert, C., Althaus, M., and Leibfritz, D. 2003. Fast proton spectroscopic imaging using steady-state free precession methods. *Magn Reson Med* **50:** 453-460.

Dreher, W., and Leibfritz, D. 2002. Fast proton spectroscopic imaging with high signal-to-noise ratio: spectroscopic RARE. *Magn Reson Med* **47:** 523-528.

Glover, G. H. 1999. 3D z-shim method for reduction of susceptibility effects in BOLD fMRI. *Magn Reson Med* **42:** 290-299.

Gruetter, R. 1993. Automatic, localized in vivo adjustment of all first- and second-order shim coils. *Magn Reson Med* **29:** 804-811.

Gruetter, R. 2002. In vivo 13C NMR studies of compartmentalized cerebral carbohydrate metabolism. *Neurochem. Int.* **41:** 143-154.

Gruetter, R., Adriany, G., Choi, I. Y., Henry, P. G., Lei, H., and Oz, G. 2003. Localized in vivo 13C NMR spectroscopy of the brain. *NMR Biomed.* **16:** 313-338.

Gruetter, R., Seaquist, E. R., Kim, S., and Ugurbil, K. 1998a. Localized in vivo ^{13}C-NMR of Glutamate Metabolism in the Human Brain: Initial Results at 4 Tesla. *Dev. Neurosci.* **20:** 380-388.

Gruetter, R., and Tkac, I. 2000. Field mapping without reference scan using asymmetric echo-planar techniques. *Magn Reson. Med.* **43:** 319-323.

Gruetter, R., Weisdorf, S. A., Rajanayagan, V., Terpstra, M., Merkle, H., Truwit, C. L., Garwood, M., Nyberg, S. L., and Ugurbil, K. 1998b. Resolution improvements in in vivo ^{1}H NMR spectra with increased magnetic field strength. *J Magn. Reson.* **135:** 260-264.

Henry, P. G., Oz, G., Provencher, S., and Gruetter, R. 2003a. Toward dynamic isotopomer analysis in the rat brain in vivo: automatic quantitation of 13C NMR spectra using LCModel. *NMR Biomed.* **16:** 400-412.

Henry, P. G., Tkac, I., and Gruetter, R. 2003b. 1H-localized broadband 13C NMR spectroscopy of the rat brain in vivo at 9.4 T. *Magn Reson Med* **50:** 684-692.

Hiba, B., Faure, B., Lamalle, L., Decorps, M., and Ziegler, A. 2003. Out-and-in spiral spectroscopic imaging in rat brain at 7 T. *Magn Reson Med* **50:** 1127-1133.

Hiba, B., Serduc, R., Provent, P., Farion, R., Remy, C., and Ziegler, A. 2004. 2D *J*-resolved Spiral Spectroscopic Imaging at 7 T: Application to Mobile Lipid Mapping in a Rat Glioma. *Magn Reson Med* **52:** in print.

Juchem, C., Merkle, H., Logothetis, N. K., and Pfeuffer, J. 2004. In vivo CSI of glutamate in Macaca mulatta brain. *Proc. , ISMRM, 12th Scientific Meeting, Tokyo.* p. 32.

Mayer, D., Dreher, W., and Leibfritz, D. 2004. Fast correlation peak imaging using spectroscopic RARE and circularly reduced chemical shift encoding. *Proc. , ISMRM. , 11th. Scientific. Meeting. , Toronto.* p. 1125.

Pan, J. W., Stein, D. T., Telang, F., Lee, J. H., Shen, J., Brown, P., Cline, G., Mason, G. F., Shulman, G. I., Rothman, D. L., and Hetherington, H. P. 2000. Spectroscopic imaging of glutamate C4 turnover in human brain. *Magn Reson Med* **44:** 673-679.

Pan, J. W., Twieg, D. B., and Hetherington, H. P. 1998. Quantitative spectroscopic imaging of the human brain. *Magn Reson Med* **40:** 363-369.

Pfeuffer, J., Tkac, I., Choi, I. Y., Merkle, H., Ugurbil, K., Garwood, M., and Gruetter, R. 1999a. Localized in vivo 1H NMR detection of neurotransmitter labeling in rat brain during infusion of [1-13C] D-glucose. *Magn Reson Med.* **41:** 1077-1083.

Pfeuffer, J., Tkac, I., Provencher, S. W., and Gruetter, R. 1999b. Toward an in vivo neurochemical profile: quantification of 18 metabolites in short-echo-time ^{1}H NMR spectra of the rat brain. *J Magn Reson* **141:** 104-120.

Scheenen, T. W., Klomp, D. W., Roll, S. A., Futterer, J. J., Barentsz, J. O., and Heerschap, A. 2004. Fast acquisition-weighted three-dimensional proton MR spectroscopic imaging of the human prostate. *Magn Reson Med* **52:** 80-88.

Thelwall, P. E., Blackband, S. J., and Chen, W. 2003. Field dependence of 17O T1, T2 and SNR - in vitro and in vivo studies at 4.7, 11, and 17.6 Tesla. *Proc. , ISMRM, 11th Scientific Meeting, Toronto.* p. 504.

Tkac, I., Andersen, P., Adriany, G., Merkle, H., Ugurbil, K., and Gruetter, R. 2001. In vivo 1H NMR spectroscopy of the human brain at 7 T. *Magn Reson Med* **46:** 451-456.

Ugurbil, K., Adriany, G., Andersen, P., Chen, W., Garwood, M., Gruetter, R., Henry, P. G., Kim, S. G., Lieu, H., Tkac, I., Vaughan, T., Van De Moortele, P. F., Yacoub, E., and Zhu, X. H. 2003. Ultrahigh field magnetic resonance imaging and spectroscopy. *Magn Reson Imaging* **21:** 1263-1281.

Ugurbil, K., Adriany, G., Andersen, P., Chen, W., Gruetter, R., Hu, X., Merkle, H., Kim, D. S., Kim, S. G., Strupp, J., Zhu, X. H., and Ogawa, S. 2000. Magnetic resonance studies of brain function and neurochemistry. *Annu. Rev. Biomed. Eng* **2:** 633-660.

van Dorsten, F. A., Van Der, G. M., Engelbrecht, M. R., Van Leenders, G. J., Verhofstad, A., Rijpkema, M., De La Rosette, J. J., Barentsz, J. O., and Heerschap, A. 2004. Combined quantitative dynamic contrast-enhanced MR imaging and (1)H MR spectroscopic imaging of human prostate cancer. *J. Magn Reson Imaging* **20:** 279-287.

Vaughan, J. T., Garwood, M., Collins, C. M., Liu, W., DelaBarre, L., Adriany, G., Andersen, P., Merkle, H., Goebel, R., Smith, M. B., and Ugurbil, K. 2001. 7T vs. 4T: RF power, homogeneity, and signal-to-noise comparison in head images. *Magn Reson. Med.* **46:** 24-30.

Zhu, X. H., Merkle, H., Kwag, J. H., Ugurbil, K., and Chen, W. 2001. 17O relaxation time and NMR sensitivity of cerebral water and their field dependence. *Magn Reson. Med.* **45:** 543-549.

Zhu, X. H., Zhang, Y., Tian, R. X., Lei, H., Zhang, N., Zhang, X., Merkle, H., Ugurbil, K., and Chen, W. 2002. Development of (17)O NMR approach for fast imaging of cerebral metabolic rate of oxygen in rat brain at high field. *Proc. Natl. Acad. Sci. U. S. A* **99:** 13194-13199.